PRATIBHA: INTERNATIONAL JOURNAL OF SCIENCE, SPIRITUALITY, BUSINESS AND TECHNOLOGY (IJSSBT), Vol. 1, No.1, March 2012
ISSN (Print) 2277—7261

A NEW METHOD OF SPEED CONTROL OF A THREE-PHASE INDUCTION MOTOR INCORPORATING THE OVERMODULATION REGION IN SVPWM VSI

*S. K. Bhartari[1], Vandana Verma[2], Anurag Tripathi[3]**
[1,2]Author is with PSIT Engineering College, Kanpur
[3]Author is with Institute of Engineering. & Technology, Lucknow

Abstract: This paper proposes the matlab based model of a new scheme of speed control of the three phase induction motor under which the speed command is compared with the actual speed and the error is processed to generate the gating patterns for the space vector modulated voltage source inverter. The space vector modulation technique ensures linearity till an output of 90.7% of the installed inverter capacity. Beyond this value, if higher inverter output is desired, the operation is termed as overmodulation. The speed control scheme incorporates the two reported regions of overmodulation i.e. I & II and ensures a smooth transition of the motor till 100% of its rated speed and also beyond that in the field weakening region. Overmodulation is a non-linear process, and it involves two modes of operation depending on modulation index (MI). Mode I provides compensation of the voltage vector to be applied while mode II uses the concept of continuous application of a particular voltage vector in order to achieve the desired average voltage vector and hence angular velocity. In this paper, the range of mode I operation of overmodulation is extended beyond usual modulation index thus far reported (0.9535) in the literature, thus stretching the arrival of Mode II further towards six step. This delay in the arrival of overmodulation Mode II reduces the non-linearity effect as the lower order harmonics are minimized, thereby enhancing the controllability of the motor angular velocity. This helps in mitigating the current and torque ripples in the motor. The satisfactory operation of the extended range of mode I and the smooth transition into mode II and six step is verified using simulation results.

Keywords: Overmodulation, SVPWM, Volt–Second compensation.

I. INTRODUCTION

The basic advantage of SVPWM is that it increases the linear range of operation till a modulation index of 90.7% unlike the conventional sine PWM method having linear range till a modulation index of 78.5%. The concept of operation of linear or non-linear region is based on modulation index that indirectly provides information about the inverter utilization capability. . This feature of SVPWM puts on edge over other PWM techniques. Till M I $\leq$ 0.907 SVPWM inverter operates in the linear region meaning whereby that the modulation index is directly proportional to the fundamental component of the line side voltage. Beyond M I = 0.907 SVPWM inverter stands operating in the non-linear or in other words overmodulation region. This overmodulation region is further divided into two zones. Zone 1 lies between 0.907 < M I $\leq$ 0.9535 and zone II lies between 0.9535 < M I $\leq$ 1.0.

The main aim of any PWM technique is to utilize the inverter to its full capacity that is achieved only with six-step operation but at the cost of loss of controllability. In SVPWM, the operation from under modulation to overmodulation finally leads to the six-step operation.

The normal and six-step operating regions of a modulator can be easily programmed, but to maintain continuity between these two regions, overmodulation is required. Besides this, overmodulation helps in exploiting the voltage capability of the inverter and therefore is necessary to improve the dynamic response of the drive. To this end, several methods of achieving overmodulation are suggested.

In [1], the overmodulation range is divided into two sub-regions and the inverter switching is defined based upon the unique characteristics

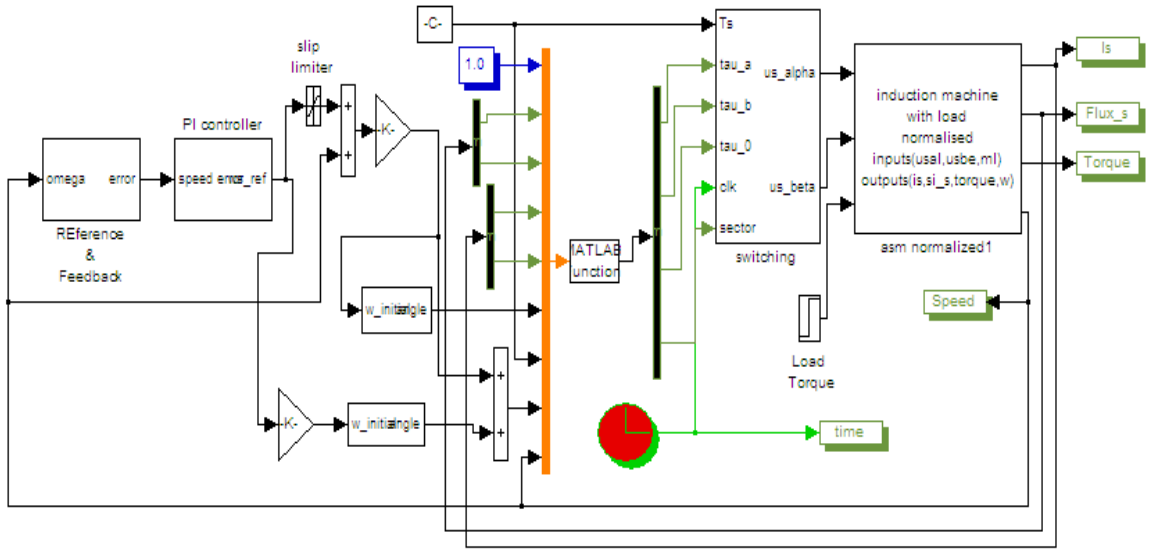

Figure 1: The complete SVM scheme applied to a three phase Induction motor

of the two regions. In the first sub-region, a pre-processor modifies the magnitude of the reference voltage vector before the conventional space vector modulator processes it. In the second sub-region, the pre-processor modifies both the angle and magnitude of the reference voltage vector. To avoid the solution of nonlinear equations, two look up tables are used and continuous control of voltage is obtained until six-step region. While the fundamental voltage cannot be obtained in every sampling period, [1] gets it in a fundamental cycle. The other overmodulation schemes like [2],[3],[4], [5] use the basic geometrical understanding provided in [1]. However, these methods differ from each other in the manner they implement the overmodulation switching strategy. In terms of minimum processing time, the method given in [4] is the fastest. However, due to large harmonic content in the voltage waveform, it results into distorted current and flux waveforms. The method described in [2] uses computationally intensive classification algorithms to achieve overmodulation. Instead of pre-processing the voltage vector as in [1], references [3] and [5] use approximated piecewise linearized equations to achieve overmodulation switching. All these methods have effectively extended the DC-bus utilization of the inverter until the six-step mode and are tested for the open loop V/f drives. During overmodulation, lower order harmonics are added to improve the fundamental cycle voltage gain of the modulator. However, when used in a closed loop torque and flux vector control scheme like FOC, these harmonics interfere with the working of linear current controllers, [6]. In reference [6], a method of compensation is proposed that uses an inverse model to estimate the harmonic component of the current vector during overmodulation. This harmonic content is then discarded from the inputs to the linear controllers. During dynamics at high angular velocities, the method developed by Mochikawa et al. selects the voltage vector that is vectorially closest to the reference [7]. This is achieved by projecting the reference voltage vector tip point on the closest inverter hexagon side. Another method implemented by Seidl et al. [8], uses neural networks for implementation, [7]. This approach however fails to utilize the voltage capability and requires a computationally intensive control algorithm. In the reference [9] an attempt is made to overcome the adverse effect of the nonlinear gain on the linear current controllers by utilizing the nonlinear inverter gain function model. This method appears to give a performance that is similar to a much simpler approach using look-up tables that are proposed in [1].

Besides the SVM based overmodulation methods discussed in the above paragraphs, a class of discontinuous PWM methods [10] have been described that extend the linear range of operation using the sine-triangle PWM scheme. In this category, the popular methods tested for V/f induction motor drives are the one by Ogasawara [11]. A hybrid method that combines the advantages of these methods is developed in [10]. However, the steady state FOC drive performance

using these methods in the overmodulation range is shown to be oscillatory.

II. CONTRIBUTION AND ORGANIZATION OF THE PAPER:

The proposed strategy of extending the range of overmodulation zone I and further achieving a smooth transition to overmodulation II and six step, considers the instantaneous value of stator voltage vector. The gating pattern is generated by the sampled error between the reference voltage vector and the estimated or actual voltage vector. Consideration of stator voltage vector error as the commanded value helps to achieve zero flux vector error in a fundamental cycle for all operating angular velocities. Figure 1 shows the complete scheme for the speed control of the three phase Induction motor.The achievement of the increased MI for zone I overmodulation, carried out right from the fundamental principle of calculating the switching times and selection of switching states is discussed in this paper. The mathematical equations developed are simulated through MATLAB / SIMULINK and the results of simulations are then validated through experimental results.

III. SPACE VECTOR MODULATION TECHNIQUE:

The figure 2 shows the three modes of operation of SVPWM. The operation within the inscribed circle of the regular hexagon is the linear region while operation outside the inscribed circle till the circumscribed circle around the hexagon depicts overmodulation region.

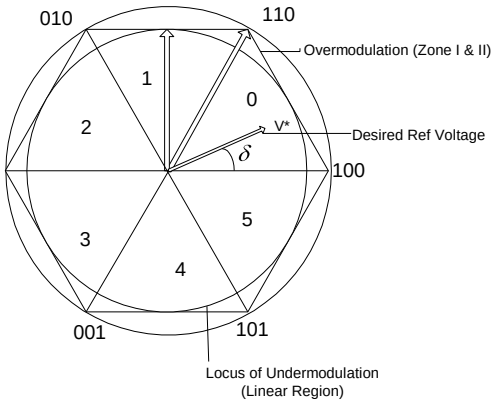

Figure 2: Showing the various regions of modulation

At the end of the liner modulation i.e. at a MI >0.907, the reference voltage vector tip traces a circle whose radius becomes greater than that of the inscribed circle of the hexagon representing the voltage vectors which can be applied in the six sectors.

IV. OVERMODULATION (ZONE I)

As can be seen from the figure 3, the whole situation in the OVMI stage can be divided into two regions. In region A, the value of the (desired) reference voltage vector $V_s^*(k)$ i.e. OD, is more than the actual available voltage vector $V_s(k)$ i.e. OC, which in region B is the other way round.

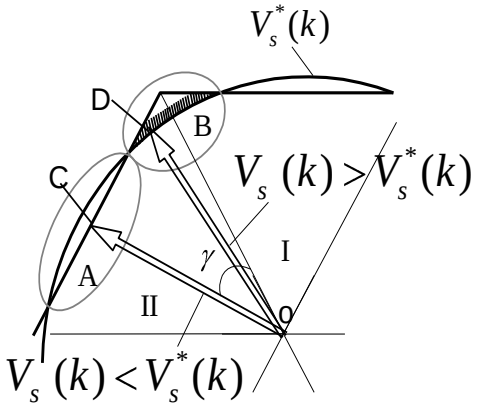

Figure 3: Overmodulation compensation

In region A, the maximum available reference voltage vector is $0.866 \times V_s(k)_{\max}$. So,

Max loss (of volt-sec) in region A =

$$V_s^*(k) - 0.866 \times V_s(k)_{\max} \quad (1)$$

Among the switching times τau_a, τau_b, and τau_0, τau_0 becomes negative in region A, which is not possible practically, so τau_0 is taken to be equal to zero and the switching is obtained by applying active states for τau_a and τau_b period only. The voltage vector in this region thus moves along the hexagon till the boundary of the region B starts.

In the region B, there is an ample available voltage vector $V_s(k)$ magnitude to accommodate tau_0 so all the three switching times are applied albeit in a modified manner. The loss of angular velocity in the region A is compensated in the region B. This compensation results in the modification of the switching times.

$$\text{Max.compensation} = k_c \times V_s(k)_{\max} - V_s^*(k) \quad (2)$$

Where k_c is a compensation factor which decides what percentage of the maximum voltage vector

ought to be required to compensate for the loss of angular velocity in the region A. Thus equating (1) and (2),

$$V_s^*(k) - 0.866V_s(k)_{\max} = k_c \times V_s(k)_{\max} - V_s^*(k) \quad (3)$$

This gives

$$k_c = \frac{2V_s^*(k)}{V_s(k)_{\max}} - 0.866$$

The rationale of the proposed method lies in the fact that since negative values of τau_0 are not possible to achieve in the region A, the value of τau_0 is kept zero in this region and only the two active voltage vectors are switched. The accompanying loss in the volt-seconds has to be compensated and this is done in the region B where the values of τau_a & τau_b have to be increased by applying the factor Kc, which is decided by equating the maximum loss (of volt-sec) in the region A with the maximum possible value of compensation that can be provided in the region B. Thus the average angular velocity can be made equal to the desired (reference) value in a sector rather than that in a complete cycle. It has been found that the modulation index at which negative values of τau_0 start occurring (during simulation) is the value at and beyond which compensation for the loss of volt-sec in the region A cannot be done.

The modified switching times are
τau_a1 = τau_a + 0.5 K_C *τau_0
τau_b1 = τau_b + 0.5K_C *τau_0
τau_01 = Ts – τau_a1 – τau_b1

The simulated results with the above switching times show that the overmodulation I region persists beyond a modulation index of 0.9535.

V. SIMULATION RESULTS AND DISCUSSION

The simulated results using MATLAB/SIMULINK are given in figures 4, 5 and 6. Typical values of MI=0.9535, 0.97 and 0.99 are considered for showing the difference in the various waveforms from the usual limit of overmodulation Zone I i.e. MI= 0.9535.

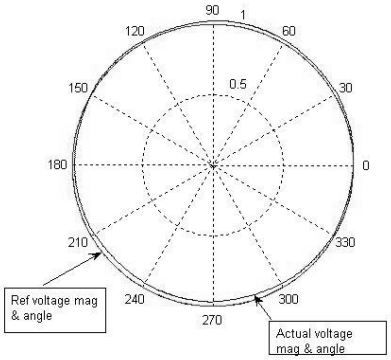

Figure 4(a)

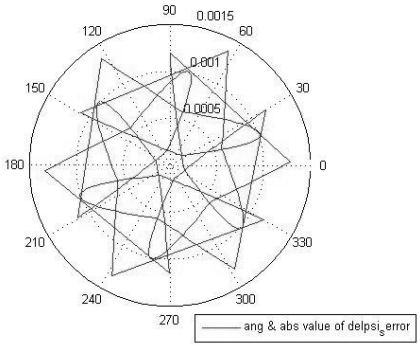

Figure 4(b)

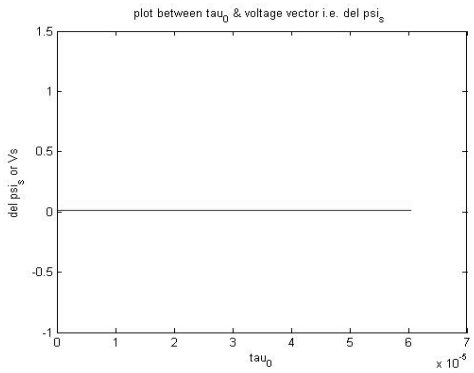

Figure 4(c)

The polar plots of voltages (both reference and actual) are shown in Figures 4(a), 5(a), 6(a) for MI = 0.9535, 0.97 and 0.99 respectively. Among the above modulation indices, that of MI=0.9535 is the existing value of MI which demarcates overmodulation zone I and zone II. Figure 4(a) proves that the actual value of voltage vector strictly tries to follow the reference voltage vector. Figure 4(b) shows that the flux error vector (which is actually equal to the applied voltage vector), is well within the normalized value of 0.0157. The same will be depicted for MI = 0.97 in Figure 5(a) where the maximum loss in actual voltage vector is successfully compensated by the maximum available voltage vector at the vertices of the hexagon. The same control and compensation is not possible for MI = 0.99 as is clear from figure

6(a). Here, clearly overmodulation Zone II exists and a continuous switching of a single voltage vector control technique are adopted to finally reach to six-step voltage level.

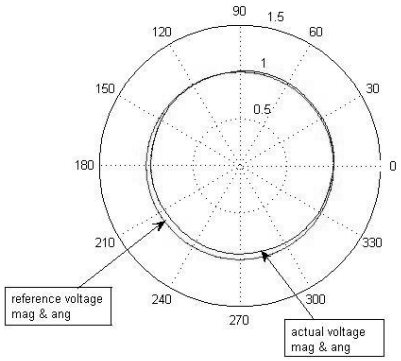

Figure 5(a)

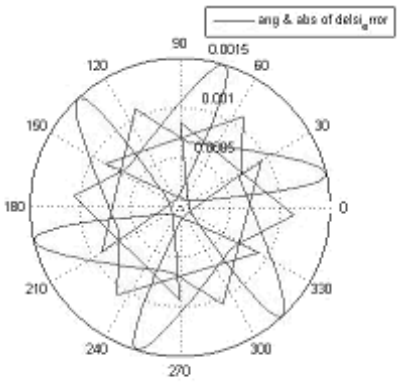

Figure 5(b)

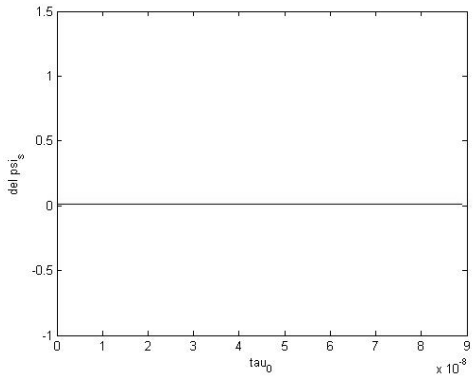

Figure 5(c)

Figures 5 (a-b) show the plots of same parameters considered in figure 4 but for MI = 0.97. Figures 4 (a, b) and figures 5(a, b) reflect the difference in value of magnitude of actual voltage vector. The increased value of voltage vector in figure 5(b) is still within the range where compensation is possible, whereas in figure 6(b) for MI=0.99 the magnitude of voltage vector crosses the boundary of the desired value and thus loses control through compensation process.

In figures 4(c), 5(c) and 6(c) the plots of voltage vectors verses zero switching times i.e. τau_0 are presented. In figure 4(c) the τau_0 = 60 microseconds. In figure 5(c) τau_0=0.09 microseconds and in figure 6(c) τau_0= a negative value. As can be seen that till modulation index of 0.97,the value of τau_0 is positive meaning that the compensation of the voltage vectors is still possible. For higher values of modulation index, overmodulation II region sets in. Thus we see that the arrival of overmodulation II is stretched further towards six step.

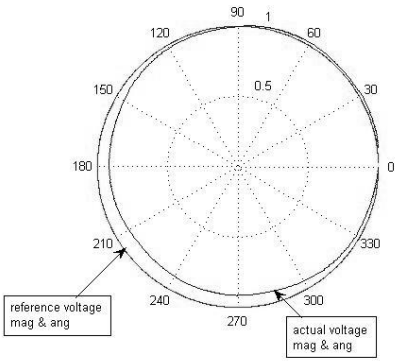

Figure 6(a)

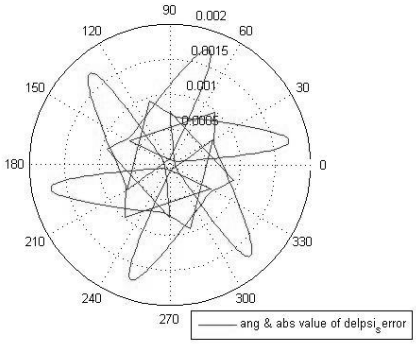

Figure 6(b)

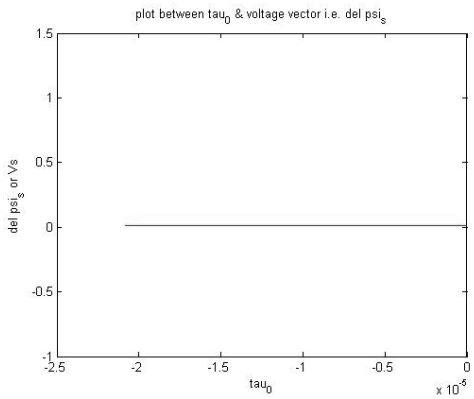

Figure 6(c)

The negative values of τau_0 directly reflect the zone of operation in overmodulation II region in SVPWM inverter. Since τau_0 cannot be negative so is kept zero and the control is achieved through active state vectors. Thus, the overmodulation zone II operation starts. The simulated results in figures 4(c), 5(c) and 6(c) define and conclude the extended range of operation of Zone I in overmodulation region.

The smooth control of torque and speed of three-phase induction motor is easily possible now with extended range of overmodulation Zone I. This gives greater flexibility in obtaining the required input voltage of the motor from the SVPWM inverter by generating the gating signals accordingly. It also helps in better and smooth transition from overmodulation to six-step operation. Moreover, extended range of Zone I improve the transient response of the torque and speed of the induction motor by reducing the pulsations in the torque in the dynamic condition.

VI. CONCLUSION

The novel approach towards the achievement of extended range of Zone I overmodulation presented in this paper when realized through simulations show the improved transient response of the induction motor with less effect of non linearity faced during overmodulation operation in SVPWM inverter. Since the Zone I range is stretched beyond the existing value of MI=0.9535, in turn, automatically reduces the range of operation in Zone II i.e. now zone II region starts at a much later value of MI. Hence, the control and transition to six step operation of the required voltage vector is much easy and even. The proposed approach removes the problem arising out of the extreme non linearity starting with the advent of overmodulation zone II by increasing the range of operation of zone I

REFERENCES

[1] J. Holtz, W. Lotzkat, and A. M. Khambadkone, "On continuous control of pwm inverters in overmodulation range including six-step," IEEE Transaction on Power Electronics, vol. 8, pp. 546–553, 1993.

[2] A. R. Bakhshai, G´eza, Jo´os, P. K.Jain, and H. Jin, "Incorporating the overmodulation range in space vector pattern generators using a classification algorithm,"
IEEE Trans. on Power Electronics, vol. 15, pp. 83 – 91, January 2000.

[3] D.-C. Lee and G.-M. Lee, "A novel overmodulation technique for space-vector pwm inverters," IEEE Trans. on Power Electronics, vol. 13, no. 6, pp. 1144–1151, 1998.

[4] S. Bolognani and M.Zigliotto, "Novel digital continuous control of svm inverters in the overmodulation range," IEEE Trans. on Industrial Applications, vol. 33, no. 2, pp. 525–530, 1997.

[5] G. Narayanan and V. T. Ranganathan, "Overmodulation algorithm for space vector modulated inverters and its application to low switching frequency pwm techniques," in Electric Power Applications, IEE Proceedings, vol. 148, November 2001.

[6] A. M. Khambadkone and J. Holtz, "Current control in overmodulation range for space vector modulation based vector controlled induction motor drives,"
(Nagoya, Japan), pp. 1334–1339, October 2000.

[7] H. Mochikawa, T. Hirose, and T. Umemoto, "Overmodulation of voltage source pwm inverter," in JIEE-Ind Society conference records, 1991.

[8] D. R. Seidl, D. A. Kaiser, and R. D. Lorenz, "One-step optimal space vector pwm current regulation using a neural network," in IEEE-Industrial Application Soc. Conf. Rec., 1994.

[9] R. J. Kerkman, T. M. Rowan, D. Leggate, and B. J. Seibel, "Control of pwm voltage inverters in pulse dropping range," IEEE Industry Application Magazine, vol. 2, pp. 24–31, Sept-Oct 1996.

[10] A. M. Hava, R. J. Kerkman, and T. A. Lipo., "Carrier-based PWM-VSI overmodulation strategies: analysis, comparison, and design," IEEE Transactions on Power Electronics, vol. 13, pp. 674–689, July 1998.

[11] S. Ogasawara, H. Akagi, and A. Nabae, "A novel PWM scheme of voltage source inverter based upon space vector theory," in European Power Electronics Conference records, 1989.